Combining the Entropy Method and Genetic Algorithm in the Multi-Objective Grinding Process

Nguyen Trong Mai
Hanoi University of Industry, Hanoi-100000, Vietnam
nguyentrongmai@haui.edu.vn (corresponding author)

Received: 21 January 2025 | Revised: 09 February 2025 | Accepted: 14 February 2025

 DOI: https://doi.org/10.48084/etasr.10312

ABSTRACT

Grinding is a commonly used method for machining products that require high precision in the mechanical engineering industry. This study conducts multi-objective optimization of the grinding process for SUS440C steel on a surface grinding machine. A total of 15 experiments were designed by deploying the Box-Behnken method. In each experiment, the values of three cutting parameters, namely workpiece speed, feed rate, and depth of cutting, varied, while four objectives, involving surface roughness (*Ra*), cutting force component in the x-direction (*Fx*), cutting force component in the y-direction (*Fy*), and cutting force component in the z-direction (*Fz*), were measured. The entropy method was used to calculate the weights of the objectives, and the Genetic Algorithm (GA) was employed to solve the multi-objective optimization problem. According to the results, the optimal values of 5 m/min, 3 mm/stroke, and 0.0198 mm were, respectively, obtained for the workpiece speed, feed rate, and depth of cut. Corresponding to these cutting parameter optimal values, the values attained for the *Ra*, *Fx*, *Fy*, and *Fz* objectives were 0.612 mm, 10.126 N, 13.621 N, and 4.112 N, respectively.

Keywords-surface grinding; SUS440C steel; multi-objective optimization; entropy method; genetic algorithm

I. INTRODUCTION

Grinding is a widely deployed machining process in mechanical manufacturing, particularly for producing high-precision components [1-4]. However, its optimization is essential to fully leverage its benefits [5-7]. Numerous studies have focused on multi-objective optimization to ensure that various process parameters simultaneously achieve their desired values [8, 9]. Researchers have applied different algorithms to solve these optimization problems and have implemented various methods to determine objective weights. Given that a comprehensive review of all published research is not feasible, authors in [10] highlight some of the most recent and relevant works on the topic. The Neumaier algorithm, integrated into the DESIGN EXPERT V7.1.3 software, was utilized to optimize the multi-objective grinding process of EN-8 steel in an attempt to simultaneously ensure the lowest surface roughness and highest material removal rate, with the weights of these two criteria having been equally chosen as 0.5 [10]. In [11], the Neumaier algorithm was also applied to optimize the multi-objective grinding process of Hardox 500 steel, and thus ensure the lowest surface roughness and highest material removal rate, with these two criteria weights having also been equally chosen. The TOPSIS algorithm was deployed to optimize the multi-objective grinding process of DIN 1.2379 steel to simultaneously ensure the lowest surface roughness, vibration of the grinding machine spindle in the x, y, and z directions, and the highest material removal rate, with the weights of the objectives having been equally chosen as 0.2 [12]. The DEAR algorithm was implemented to optimize the multi-objective grinding process of AISI 4140 steel to simultaneously ensure low surface roughness and high material removal rate, where the weights of the objectives were calculated using the DEAR algorithm itself [13]. In [14], the DEAR algorithm was also utilized to optimize the multi-objective grinding process of SAE420 steel, with the objective of simultaneously ensuring the lowest surface roughness and vibration of the grinding machine spindle in the x, y, and z directions. In [15], the weights of the objectives were calculated using the DEAR algorithm. The PSO algorithm was applied to optimize the multi-objective grinding process of D2 tool steel to simultaneously ensure the highest material removal rate and the smallest dimensional error, with the weights of these two parameters not having been clearly defined. The Desirability Functional Approach (DFA) was deployed to optimize the multi-objective grinding process of AISI 4140 steel to simultaneously ensure the lowest cutting temperature, highest material removal rate, and lowest machining cost, with the weights of these three parameters being equally chosen as 1/3 [16]. The meta-heuristic algorithm was employed to optimize the multi-objective grinding process of AISI 316 stainless steel to simultaneously ensure the lowest surface roughness, smallest shape deviation, and highest material removal rate. The weights of these three parameters were assigned according to the subjective viewpoint of the optimization problem solver [17]. Two algorithms, MOORA

and COPRAS, were implemented to optimize the multi-objective grinding process of SKD11 steel, and hence simultaneously ensure the lowest surface roughness and highest material removal rate. The weights of these two criteria were calculated using the Entropy method [18]. The GA algorithm was applied to optimize the grinding process of pinus sylvestris material to ensure the lowest surface roughness [19]. The GA algorithm was employed to optimize the multi-objective grinding process of SKD11 steel, where the weights of the three objectives, including surface roughness, grinding time, and the deviation between the actual and desired grinding depth, were equally chosen as 1/3 [20]. In [21], the GA algorithm was deployed to optimize the multi-objective grinding process when grinding BK7 optical glass, with the weights of the surface roughness and specific energy objectives having not been mentioned. A summary of the above studies shows that many different algorithms and weight calculation methods have been used to optimize the multi-objective grinding process. However, there seems to be no research integrating criterion weight calculation utilizing the Entropy method and the GA algorithm to optimize the multi-objective grinding process. This gap has motivated the conduct of the present research.

II. MATERIALS AND METHODS

A. Experimental Setup

The test specimens were made of SUS440C steel with dimensions of 50 mm, 30 mm, and 10 mm in length, width, and height, respectively. The chemical composition of some major elements of this steel type is summarized in Table I. An APSG-820/8A surface grinding machine, manufactured in Taiwan, was used to conduct the experiments. Surface roughness was measured utilizing an SJ-201 surface roughness tester, manufactured in Japan. The force components were measured using a KISTLER force transducer. Figure 1 depicts the experimental setup. To minimize the impact of random errors on the measurement results, each experiment involved calculating the response parameters, namely, surface roughness and cutting force, at least three times. The final response values for each experiment were determined by averaging the consecutive measurements.

B. Experimental Design

In the experiments, three parameters were varied: workpiece speed, feed rate, and depth of cutting. These parameters can be easily adjusted by the machine operator [22, 23]. Each cutting parameter was tested at three levels, coded as -1, 0, and +1, as shown in Table II. The values in Table I were chosen based on relevant references/research and the technological capabilities of the employed experimental machine [22, 23]. The experimental design followed a Box-Behnken approach with 15 experiments, as outlined in Table III. This design is widely applied in optimization studies and mechanical research [22, 23].

TABLE I. CHEMICAL COMPOSITION OF SUS440C STEEL

C (%)	Si (%)	Mn (%)	P (%)	S (%)	Cr (%)	Ni (%)	Mo (%)
0.95-1.20	≤ 1.00	≤ 1.00	≤ 0.04	≤ 0.03	16-18	≤ 0.06	≤ 0.75

Fig. 1. Experimental setup: (a) component, (b) force component, measurement system, (c) surface roughness measurement system.

TABLE II. INPUT PARAMETERS

Parameter	Unit	Symbol	Value at level		
			-1	0	+ 1
Workpiece velocity	m/min	v_c	5	8	11
Feed-rate	mm/stroke	f	3	5	7
Depth of cut	mm	a_p	0.01	0.015	0.02

TABLE III. EXPERIMENTAL DESIGN MATRIX

Trial.	Coden value			Real value		
	v_c	f	a_p	v_c, m/min	f, mm/stroke	a_p, mm
1	0	+1	+1	8	7	0.02
2	0	0	0	8	5	0.015
3	0	0	0	8	5	0.015
4	+1	0	+1	11	5	0.02
5	-1	-1	0	5	3	0.015
6	0	-1	-1	8	3	0.01
7	0	+1	-1	8	7	0.01
8	+1	-1	0	11	3	0.015
9	+1	0	-1	11	5	0.01
10	-1	+1	0	5	7	0.015
11	+1	+1	0	11	7	0.015
12	-1	0	-1	5	5	0.01
13	0	-1	+1	8	3	0.02
14	-1	0	+1	5	5	0.02
15	0	0	0	8	5	0.015

C. Entropy Method

Assuming that m experiments have been conducted, and n output parameters have been measured at each experiment, let x_{ij} be the value of the j^{th} output parameter at the i^{th} experiment, with j ranging from 1 to n and i from 1 to m. The weight calculation for the j^{th} parameters using the Entropy method is performed as [24-26]:

- Step 1: Determine the normalized value for each criterion according to:

$$n_{ij} = \frac{x_{ij}}{m+\sum_{i=1}^{m} x_{ij}^2} \quad (1)$$

- Step 2: Calculate the value of the entropy measure for each parameter j according to:

$$e_j = \sum_{i=1}^{m}[n_{ij} \times ln(n_{ij})] - (1 - \sum_{i=1}^{m} n_{ij}) \times ln(1 - \sum_{i=1}^{m} n_{ij}) \quad (2)$$

- Step 3: Calculate the weight for each parameter according to:

$$w_j = \frac{1-e_j}{\sum_{j=1}^{n}(1-e_j)} \quad (3)$$

D. Genetic Algorithm

The GA is an optimization search technique inspired by biological evolution. GA simulates the process of natural selection, where the fittest individuals survive and pass on their characteristics to the next generation. In GA, everyone represents a possible solution to the problem to be solved, while through generations, GA is expected to find better and better solutions. The block diagram of GA includes the following basic components [27, 28]:

- Initialization: Randomly generate an initial population of individuals.
- Evaluation: Calculate the fitness function for everyone to evaluate their suitability for the problem.
- Selection: Select individuals with high fitness to create a new generation.
- Crossover: Combine the characteristics of selected individuals to create a new offspring.
- Mutation: Randomly change some genes of the offspring to increase the diversity of the population.
- Replacement: Replace part or all the old population with the new population.
- Termination: If the termination condition is met (e.g., the maximum number of generations, the best fitness achieved), stop the algorithm, otherwise return to step 2.
- Accordingly, the block diagram of GA is presented in Figure 2 [29].

III. RESULTS AND DISCUSSION

Experiments were conducted in the sequence outlined in Table III, with the values of Ra, Fx, Fy, and Fz having been measured in each trial. Ra was selected as a key measurement parameter due to its significant impact on the product's performance, including wear resistance, chemical corrosion resistance, fatigue strength, and joint accuracy, all of which influence the product's lifespan. Additionally, the three force components, Fx, Fy, and Fz, were measured in each experiment, as they play a crucial role in determining surface waviness and the dimensional accuracy of the product [22]. The experimental results are outlined in Table IV.

TABLE IV. EXPERIMENTAL RESULTS

Trial.	Cutting parameter			Response			
	v_c (m/min)	f (mm/stroke)	a_p (mm)	Ra (μm)	Fx (N)	Fy (N)	Fz (N)
1	8	7	0.02	1.016	18.3	28.1	63.5
2	8	5	0.015	0.689	10.5	25.4	22.9
3	8	5	0.015	0.656	10.2	24.9	23.1
4	11	5	0.02	0.637	24.6	46.4	35.5
5	5	3	0.015	0.452	6.8	19.8	7.9
6	8	3	0.01	0.467	11.5	32.2	8.2
7	8	7	0.01	0.579	18.2	8.1	26.5
8	11	3	0.015	0.573	11.1	22.1	20.2
9	11	5	0.01	0.608	12.6	30.4	14.2
10	5	7	0.015	0.605	12.8	5.1	9.1
11	11	7	0.015	0.917	13.7	38.2	45.8
12	5	5	0.01	0.764	8.4	5.4	9.1
13	8	3	0.02	0.657	14.4	24.5	17.5
14	5	5	0.02	0.750	12.2	5.5	11.8
15	8	5	0.015	0.760	11.9	24.6	26.8

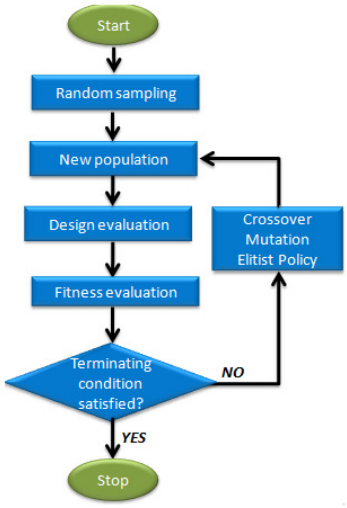

Fig. 2. Block diagram of GA.

Based on the data illustrated in Table IV, the influence of the cutting parameters on the responses was plotted, as shown in Figures 3-6. It was observed that increasing the cutting parameter values increased the surface roughness. This is consistent with the conclusions drawn in [30-32]. However, the cutting parameter influence degree on surface roughness is different. The feeding rate has the greatest impact on roughness, followed by the depth of cut, whereas the workpiece speed has the least impact on surface roughness.

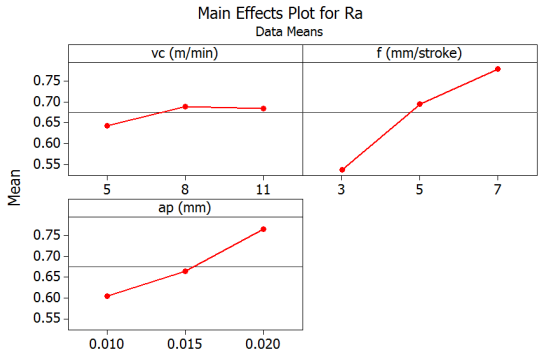

Fig. 3. Effect of cutting parameters on Ra.

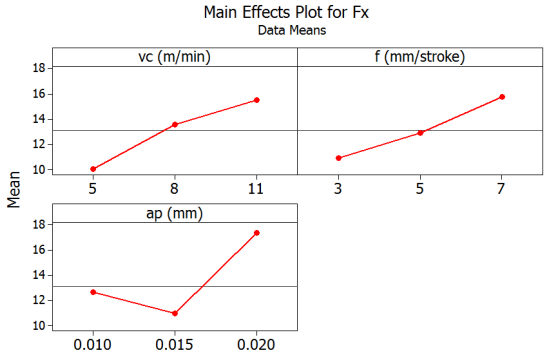

Fig. 4. Effect of cutting parameters on Fx.

For the cutting force component *Fx*, having increased the workpiece speed and feed rate increased the *Fx* value. This is also consistent with the results of [31, 32]. For the depth of cut, when it increased from 0.01 mm to 0.015 mm, *Fx* decreased. However, if the depth of cut continued to increase, *Fx* also increased. This can be explained by the fact that when the depth of cut increased from 0.01 mm to 0.015 mm, the "bonding" between the grinding wheel and the workpiece surface became stronger, causing *Fx* to decrease. However, if the depth of cut continued to increase, it would significantly increase the energy required to remove material, which is the reason for the increase in *Fx* [33].

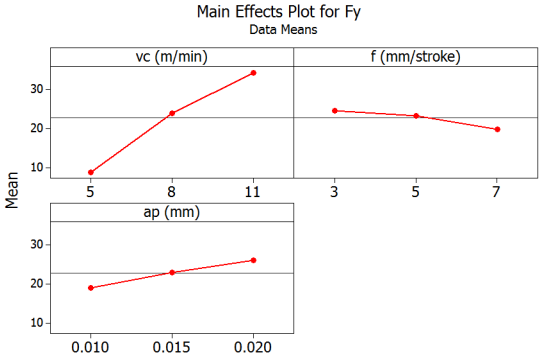

Fig. 5. Effect of cutting parameters on Fy.

Regarding *Fy*, having increased the workpiece speed and depth of cut increased the former, which is also consistent with the results of [31, 32]. Conversely, the increase in the feed rate decreased Fy, although the change in *Fy* was not significant. This can be explained by the fact that when the feed rate increased, the "re-cutting" of the abrasive grains on the workpiece surface decreased, leading to a decrease in *Fy* [34].

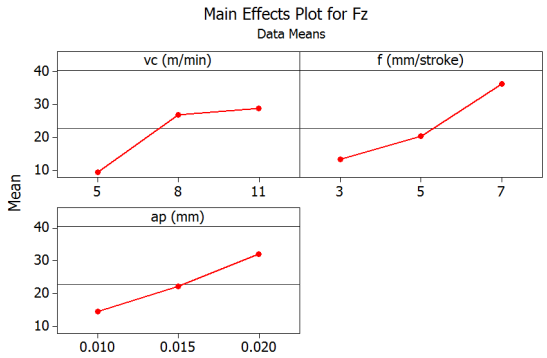

Fig. 6. Effect of cutting parameters on Fz.

As all three cutting parameters increased, the cutting force component Fz also increased. This is understandable because when the three cutting parameter values increased, the cutting depth of an abrasive grain into the workpiece surface also increased, having led to an increase in the reaction force of the workpiece surface on the grinding wheel. This, respectively, caused an increase in the cutting force perpendicular to the workpiece surface, which is the *Fz* component. This result is consistent with the findings of [31, 32]. A brief analysis of the cutting parameter influence on surface roughness and the force components *Fx*, *Fy*, and *Fz* demonstrates that it is difficult to determine the cutting parameter values to ensure that the surface roughness and all three force components *Fx*, *Fy*, and *Fz* have small values. This can be briefly explained by the following example: When machining with a small feed rate, such as 3 mm/stroke, the surface roughness and the force components *Fx* and *Fz* have also small values, but the force component *Fy* has the biggest ones. Using another example, suppose that the cutting force component *Fx* is needed to have the smallest value, then machining with a medium depth of cut, such as 0.015 mm, is required. However, at this point, both surface roughness and the two remaining cutting force components, Fy and Fz, have relatively high values. According to the aforementioned examples, to ensure that both the surface roughness and the three cutting force components have small values, it is necessary to solve the multi-objective optimization problem. To achieve this, it is first necessary to calculate the objectives' weights. Applying (1) to (3), the weights of the objectives *Ra*, *Fx*, *Fy*, and *Fz* were calculated as 0.3835, 0.2211, 0.1992, and 0.1962, respectively. The next step in multi-objective optimization is to construct a regression equation that represents the relationship between the objectives *Ra*, *Fx*, *Fy*, and *Fz* and the cutting parameters. From the experimental results evidenced in Table IV, four regression equations, (4)-(7), were respectively constructed for the four objectives *Ra*, *Fx*, *Fy*, and *Fz*. The coefficient of determination (R^2) for evaluating the accuracy of each equation has corresponding values of 0.6432, 0.8578, 0.9161, and 0.9126:

$$R_a = 0.6817 + 0.0051 \cdot v_c - 0.0021 \cdot f - 39.2083 \cdot a_p - 0.0030 \cdot v_c^2 - 0.0093 \cdot f^2 + 621.667 \cdot a_p^2 + 0.0079 \cdot v_c \cdot f + 0.7166 \cdot v_c \cdot a_p + 6.1750 \cdot f \cdot a_p \quad (4)$$

$$F_x = 33.4720 + 0.3814 \cdot v_c + 1.6541 \cdot f - 5123.33 \cdot a_p - 0.0509 \cdot v_c^2 + 0.1729 \cdot f^2 + 161667 \cdot a_p^2 - 0.1416 \cdot v_c \cdot f + 136.667 \cdot v_c \cdot a_p - 70.000 \cdot f \cdot a_p \quad (5)$$

$$F_y = 91.5095 - 1.7560 \cdot v_c - 18.8896 \cdot f - 4202.50 \cdot a_p - 0.2759 \cdot v_c^2 - 0.2958 \cdot f^2 - 22333.3 \cdot a_p^2 + 1.2833 \cdot v_c \cdot f + 265.00 \cdot v_c \cdot a_p + 692.50 \cdot f \cdot a_p \quad (6)$$

$$F_z = 51.9709 + 6.6564 \cdot v_c - 22.5250 \cdot f - 5120.00 \cdot a_p - 0.8217 \cdot v_c^2 + 0.9697 \cdot f^2 + 31166.7 \cdot a_p^2 + 1.0166 \cdot v_c \cdot f + 310.00 \cdot v_c \cdot a_p + 682.50 \cdot f \cdot a_p \quad (7)$$

The multi-objective optimization problem is expressed by (8), where w_1, w_2, w_3, and w_4 are the weights of *Ra*, *Fx*, *Fy*, and *Fz*, respectively.

To solve (8) using the GA algorithm, certain parameters needed to be defined, as displayed in Table V [35, 36]. Figure 7 presents the fitness function plot obtained when applying the GA algorithm to solve (8). The optimal value of the function f (v_c, f, a_p) along with the corresponding values of Ra, Fx, Fy, and Fz, as well as the optimal cutting parameters, are listed in Table VI.

$$\begin{cases} f(v_c, f, a_p) = w_1 \cdot R_a + w_2 \cdot F_x + w_3 \cdot F_y + w_4 \cdot F_z \rightarrow min \\ R_a, F_x, F_y, F_z > 0 \\ \begin{cases} 5\left(\frac{m}{min}\right) \le v_c \le 11\left(\frac{m}{min}\right) \\ 3\left(\frac{mm}{stroke}\right) \le f \le 7\left(\frac{mm}{stroke}\right) \\ 0.01\,(mm) \le a_p \le 0.02(mm) \end{cases} \end{cases} \quad (8)$$

TABLE V. GA PARAMETERS

Parameter	Value
Population size	150
Maximum generation	100
Crossover probability	0.25
Mutation probability	0.05
Mutation parameter	4

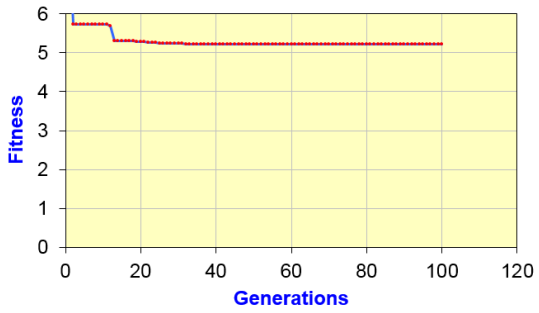

Fig. 7. Fitness function plot of f.

According to the results of the multi-objective optimization problem, the optimal values of the workpiece speed, feed rate, and depth of cut were 5 m/min, 3 mm/stroke, and 0.0198 mm, respectively. Correspondingly, the values of *Ra*, *Fx*, *Fy*, and *Fz* were 0.566 mm, 9.850 N, 11.114 N, and 3.178 N, respectively.

To verify the optimal values found by the GA algorithm, experiments were conducted on three steel samples, and the results are depicted in Table VII.

TABLE VI. OPTIMAL VALUES

Parameters	Value	Unit
v_c	5.0000	m/min
f	3.0000	mm/stroke
a_p	0.0198	mm
$f(v_c,f,a_p)$	5.231	-
Ra	0.566	μm
Fx	9.850	N
Fy	11.114	N
Fz	3.178	N

TABLE VII. EXPERIMENTAL RESULTS WITH OPTIMIZED CUTTING PARAMETERS

Test	*Ra* (μm)	*Fx* (N)	*Fy* (N)	*Fz* (N)
1	0.619	10.321	13.456	4.210
2	0.604	10.047	13.998	4.003
3	0.613	10.010	13.409	4.123

According to the experimental results, the values of *Ra*, *Fx*, *Fy*, and *Fz* were 0.612 mm, 10.126 N, 13.621 N, and 4.112 N, respectively. The experimental values of all *R*a, *Fx*, *Fy*, and *Fz* criteria were greater than those obtained by the calculated results; however, the difference was insignificant. Specifically, the difference between the calculated and experimental results was only 7.52% for *Ra*, 2.73% for *Fx*, 18.41% for *Fy*, and 22.71% for Fz.

IV. CONCLUSIONS

This study conducted a multi-objective optimization of the grinding process for SUS440C steel. The GA algorithm and Entropy weight method were combined to solve this study's grinding process optimization problem. Using the Entropy method, the weights of the criteria *Ra*, *Fx*, *Fy*, and *Fz* were calculated as 0.3835, 0.2211, 0.1991, and 0.1962, respectively. Using the GA, the optimal values of the workpiece speed, feed rate, and depth of cut were determined to be 5 m/min, 3 mm/stroke, and 0.0198 mm, respectively. Corresponding to these optimal values of the cutting parameters, the surface roughness (*Ra*) and the cutting force components *Fx*, *Fy*, and *Fz* were 0.612 mm, 10.126 N, 13.621 N, and 4.112 N, respectively. The combination of the GA algorithm and the Entropy weight method yielded highly accurate optimization results, with deviations between the calculated and experimental results of only 7.52% for *Ra*, 2.73% for *Fx*, 18.41% for *Fy*, and 22.71% for *Fz*. These results fully satisfy the accuracy requirements for solving optimization problems in machining in general and surface grinding in particular [37].

REFERENCES

[1] X. Li, Z. Tang, C. Chen, L. Wang, Y. Zhang, and D. Wang, "An optimization method of grinding wheel profile for complex large shaft curve grinding," *Journal of Advanced Manufacturing Science and Technology*, vol. 5, no. 2, Aug. 2024, Art. no. 2025008, https://doi.org/10.51393/j.jamst.2025008.

[2] D. Kumar Patel, D. Goyal, and B. S. Pabla, "Optimization of parameters in cylindrical and surface grinding for improved surface finish," *Royal Society Open Science*, vol. 5, no. 5, May 2018, Art. no. 171906, https://doi.org/10.1098/rsos.171906.

[3] D. D. Trung and N. T. Mai, "Improving the Accuracy of the Surface Roughness Model in Grinding Through Square Root Transformation," *International Journal of Mechanical Engineering and Robotics Research*, vol. 13, no. 2, pp. 249–253, 2024, https://doi.org/10.18178/ijmerr.13.2.249-253.

[4] P. Biswas *et al.*, "An Experimental Analysis of Grinding Parameters and Conditions on Surface Roughness of Finished Product," *Journal of Physics: Conference Series*, vol. 2286, no. 1, Apr. 2022, Art. no. 012027, https://doi.org/10.1088/1742-6596/2286/1/012027.

[5] A. Heininen, S. Santa-aho, J. Röttger, P. Julkunen, and K. T. Koskinen, "Grinding optimization using nondestructive testing (NDT) and empirical models," *Machining Science and Technology*, vol. 28, no. 1, pp. 98–118, Jan. 2024, https://doi.org/10.1080/10910344.2023.2296677.

[6] Vu Ngoc Pi, Luu Anh Tung, Le Xuan Hung, and Banh Tien Long, "Cost Optimization of Surface Grinding Process," *Journal of Environmental Science and Engineering A*, vol. 5, no. 12, pp. 606–611, Dec. 2016, https://doi.org/10.17265/2162-5298/2016.12A.002.

[7] S. Henkel *et al.*, "Optimization of grinding processes on fused silica components using in-process vibrometry and dynamometer measurements," *EPJ Web of Conferences*, vol. 266, 2022, Art. no. 03011, https://doi.org/10.1051/epjconf/202226603011.

[8] M. D. Abyaneh, P. Narimani, M. Hadad, and S. Attarsharghi, "Using machine learning and optimization for controlling surface roughness in grinding of St37," *ENERGY QUIPSYS*, vol. 11, no. 3, pp. 321–337, Sep. 2023.

[9] M. M. Salem, S. S. Mohamed, and A. A. Ibrahim, "Optimization of Surface Grinding Parameters Used in Improved Surface Integrity," *International Research Journal of Innovations in Engineering and Technology*, vol. 6, no. 5, pp. 124–130, May 2022, https://doi.org/10.47001/IRJIET/2022.605015.

[10] B. Dasthagiri and E. V. Goud, "Optimization Studies on Surface Grinding Process Parameters," *International Journal of Innovative Research in Science, Engineering and Technology*, vol. 4, no. 7, pp. 6148–6156, 2007.

[11] T. H. Danh and L. H. Ky, "Optimization of Wheel Dressing Technological Parameters when Grinding Hardox 500 Steel," *Engineering, Technology & Applied Science Research*, vol. 14, no. 4, pp. 15854–15859, Aug. 2024, https://doi.org/10.48084/etasr.7986.

[12] D. D. Trung, N. V. Thien, and N.-T. Nguyen, "Application of TOPSIS Method in Multi-Objective Optimization of the Grinding Process Using Segmented Grinding Wheel," *Tribology in Industry*, vol. 43, no. 1, pp. 12–22, Mar. 2021, https://doi.org/10.24874/ti.998.11.20.12.

[13] D. T. Do, X. T. Hoang, and D. H. Le, "Improving the Efficiency of Grinding Process Using the Rubber-Pasted Grinding Wheel," *Strojnícky časopis - Journal of Mechanical Engineering*, vol. 72, no. 1, pp. 23–34, May 2022, https://doi.org/10.2478/scjme-2022-0003.

[14] D. D. Trung, N.-T. Nguyen, D. H. Tien, and H. L. Dang, "A Research on Multi-Objective Optimization of the Grinding Process Using Segmented Grinding Wheel by Taguchi-Dear Method," *EUREKA: Physics and Engineering*, no. 1, pp. 67–77, Jan. 2021, https://doi.org/10.21303/2461-4262.2021.001612.

[15] Z. Chen *et al.*, "The optimization of accuracy and efficiency for multistage precision grinding process with an improved particle swarm optimization algorithm," *International Journal of Advanced Robotic Systems*, vol. 17, no. 1, Jan. 2020, Art. no. 1729881419893508, https://doi.org/10.1177/1729881419893508.

[16] R. Roy *et al.*, "Multi-Response Optimization of Surface Grinding Process Parameters of AISI 4140 Alloy Steel Using Response Surface Methodology and Desirability Function under Dry and Wet Conditions," *Coatings*, vol. 12, no. 1, Jan. 2022, Art. no. 104, https://doi.org/10.3390/coatings12010104.

[17] R. Rekha, N. Baskar, M. R. A. Padmanaban, and A. Palanisamy, "Optimization of cylindrical grinding process parameters using meta-heuristic algorithms," *Indian Journal of Engineering and Materials Sciences (IJEMS)*, vol. 27, no. 2, pp. 389–395, Mar. 2021, https://doi.org/10.56042/ijems.v27i2.45971.

[18] N.-T. Nguyen and D. D. Trung, "Combination of Taguchi method, MOORA and COPRAS techniques in multi-objective optimization of surface grinding process," *Journal of Applied Engineering Science*, vol. 19, no. 2, pp. 390–398, 2021, https://doi.org/10.5937/jaes0-28702.

[19] A. Gürgen *et al.*, "Optimization of CNC operating parameters to minimize surface roughness of Pinus sylvestris using integrated artificial neural network and genetic algorithm," *Maderas. Ciencia y tecnología*, vol. 24, 2022, https://doi.org/10.4067/s0718-221x2022000100401.

[20] V. Nguyen, D. Nguyen, D. Do, and T. Tran, "Multi-Objective Optimization of the Surface Grinding Process for Heat-Treated Steel," *International Journal of Automotive and Mechanical Engineering*, vol. 21, no. 4, pp. 11831–11843, Dec. 2024, https://doi.org/10.15282/ijame.21.4.2024.8.0911.

[21] G. Xiao, S. Yang, W. Wang, and Z. Yang, "Parameter Optimization and Experimental Study of Orderly Arrangement Grinding Wheel," *International Journal of Mechatronics and Applied Mechanics*, vol. I, no. 17, pp. 77–86, Sep. 2024, https://doi.org/10.17683/ijomam/issue17.9.

[22] N.-T. Nguyen, D. D. Trung, N.-T. Nguyen, and D. D. Trung, "A study on the surface grinding process of the SUJ2 steel using CBN slotted grinding wheel," *AIMS Materials Science*, vol. 7, no. 6, pp. 871–886, 2020, https://doi.org/10.3934/matersci.2020.6.871.

[23] D. D. Trung, "Influence of Cutting Parameters on Surface Roughness in Grinding of 65G Steel," *Tribology in Industry*, vol. 43, no. 1, pp. 167–176, Mar. 2021, https://doi.org/10.24874/ti.1009.11.20.01.

[24] D. D. Trung, "A combination method for multi-criteria decision making problem in turning process," *Manufacturing Review*, vol. 8, p. 26, Dec. 2021, https://doi.org/10.1051/mfreview/2021024.

[25] D. D. Trung and H. X. Thinh, "A multi-criteria decision-making in turning process using the MAIRCA, EAMR, MARCOS and TOPSIS methods: A comparative study," *Advances in Production Engineering & Management*, vol. 16, no. 4, pp. 443–456, Dec. 2021, https://doi.org/10.14743/apem2021.4.412.

[26] E. K. Zavadskas and V. Podvezko, "Integrated Determination of Objective Criteria Weights in MCDM," *International Journal of Information Technology & Decision Making*, vol. 15, no. 02, pp. 267–283, Mar. 2016, https://doi.org/10.1142/S0219622016500036.

[27] S. Katoch, S. S. Chauhan, and V. Kumar, "A review on genetic algorithm: past, present, and future," *Multimedia Tools and Applications*, vol. 80, no. 5, pp. 8091–8126, Feb. 2021, https://doi.org/10.1007/s11042-020-10139-6.

[28] S. R. ABBAS, "Genetic Algorithm and Particle Swarm Optimization Techniques in Multimodal Functions Optimization," MS Thesis, Near East University, Nicosia, 2017.

[29] H. K. Nguyen, P. V. Dong, and V. Q. Tran, "Investigation of influence of grinding wheel and cutting parameters on surface roughness and surface hardening when relieving grinding the gear milling teeth surface based on the Archimedes' spiral," *International Journal of Metrology and Quality Engineering*, vol. 14,Art. no. 1, 2023 https://doi.org/10.1051/ijmqe/2022016.

[30] M. Aravind and S. Periyasamy, "Optimization of Surface Grinding Process Parameters By Taguchi Method And Response Surface Methodology," *International Journal of Engineering Research*, vol. 3, no. 5, pp. 1721–1727, 2014.

[31] S. Malkin and C. Guo, *Grinding Technology: Theory and Application of Machining with Abrasives*. Industrial Press Inc., 2008.

[32] I. D. Marinescu, M. P. Hitchiner, E. Uhlmann, W. B. Rowe, and I. Inasaki, *Handbook of Machining with Grinding Wheels*. CRC Press, 2016.

[33] T. Yin, H. Zhang, W. Hang, and S. To, "A Novel Approach to Optimizing Grinding Parameters in the Parallel Grinding Process," *Processes*, vol. 12, no. 3, Mar. 2024, Art. no. 493, https://doi.org/10.3390/pr12030493.

[34] W. Kacalak, D. Lipiński, and F. Szafraniec, "Selected Aspects of Precision Grinding Processes Optimization," *Materials*, vol. 17, no. 3, Jan. 2024, Art. no. 607, https://doi.org/10.3390/ma17030607.

[35] N. T. Mai, T. D. Quy, and N. V. Manh, "Optimizing Cutting Parameters for Surface Grinding of SUS440C Steel," *International Research Journal of Advanced Engineering and Science*, vol. 9, no. 4, pp. 351–354, 2024.

[36] P. B. Khoi, D. D. Trung, N. Cuong, and N. D. Man, "Research on Optimization of Plunge Centerless Grinding Process using Genetic Algorithm and Response Surface Method," *International Journal of Scientific Engineering and Technology*, vol. 4, no. 3, pp. 207–211, Mar. 2015, https://doi.org/10.17950/ijset/v4s3/319.

[37] N. T. Binh, *Optimizing the Metal Cutting Process.* Education Publishing House, 2013.